



Numerical Analysis of Steel I-Core Sandwich Panels Subjected to Multiple Consecutive Blast Scenarios

F. Kiakojouri¹ · M. R. Sheidaii¹

Received: 4 August 2016 / Accepted: 11 September 2018 / Published online: 18 September 2018
© Shiraz University 2018

Abstract

The nonlinear dynamic response of steel I-core sandwich panels under three multiple consecutive blast scenarios using five different explosive charges has been numerically investigated. The obtained results are compared with available experimental data to verify the developed finite element model, and good agreement is observed. Special emphasis is placed on the evaluation of maximum displacements of cover plates and energy dissipation of different parts of the panels. According to the results, sandwich panels show better performance than equivalent solid plate with the same mass and material when subjected to consecutive blasts. Overall responses of panels are dependent on not only blast pressure, but also the sequence of loading. In this regard, three different phases of deformation based on blast pressure and sequence are observed in the response of panels when subjected to multiple blasts.

Keywords Blast · Sandwich panel · Nonlinear dynamic analysis · Energy dissipation

1 Introduction

Sandwich structures are of interest in different applications such as marine, protective structures, military, aerospace and transportation due to their high strength-to-weight ratio. These structures are especially effective under dynamic loads such as blast and impact because of their excellent energy dissipation capacity, and therefore, researchers have focused on the response of such structures under blast loads particularly in the last decade. Traditionally, most of these studies are experimental, but in recent years development and availability of powerful processors and finite element analysis packages facilitated the numerical study of blast-loaded sandwich structures.

In general, research works on blast-loaded metallic sandwich panels can be categorized in experimental (Rathbun et al. 2006; Zhu et al. 2008; Nurick et al. 2009), experimental–numerical (Shim et al. 2013; Yazici et al. 2014; Schiffer and Tagarielli 2014; Li et al. 2014; Arora et al. 2017), numerical (Zhu et al. 2009; Remennikov and

Kong 2012; Vatani Oskouei and Kiakojouri 2015; Ebrahimi et al. 2016; Zhang et al. 2017) and analytical studies (Fleck and Deshpande 2004; Fatt and Palla 2009; Andrews and Moussa 2009). In most of the published numerical study of blast-loaded sandwich panels, commercial finite element packages were used such as Abaqus (Yazici et al. 2014; Schiffer and Tagarielli 2014; Vatani Oskouei and Kiakojouri 2015; Ebrahimi et al. 2016; Arora et al. 2017), AUTODYN (Li et al. 2014) and LS-DYNA (Zhu et al. 2009; Remennikov and Kong 2012; Shim et al. 2013; Zhang et al. 2017).

Blast tests to study the behavior of metallic honeycomb sandwich panels were reported by Dharmasena et al. (2008). Tests were performed at three levels of explosive charges on the sandwich panels and solid plates with the same weight and material. According to results, at the lowest intensity, considerable front cover plate bending and cell buckling were observed at the midpoint of the panels closest to the blast source. The honeycomb sandwich panels suffered significantly less back face deflections than solid plates of equal weight (Dharmasena et al. 2008).

The response of metallic trapezoidal corrugated core sandwich panels under blast is experimentally studied by Zhang et al. (2015). Results showed that the displacement and damage of sandwich panel increased with the decrease

✉ M. R. Sheidaii
m.sheidaii@urmia.ac.ir

¹ Department of Civil Engineering, Urmia University, Urmia, Iran

Fig. 1 Numerical models: **a** model 1 and **b** model 2

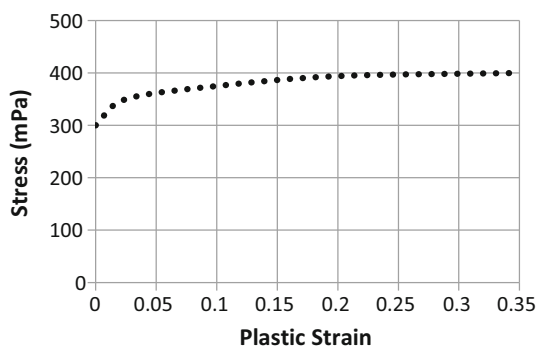
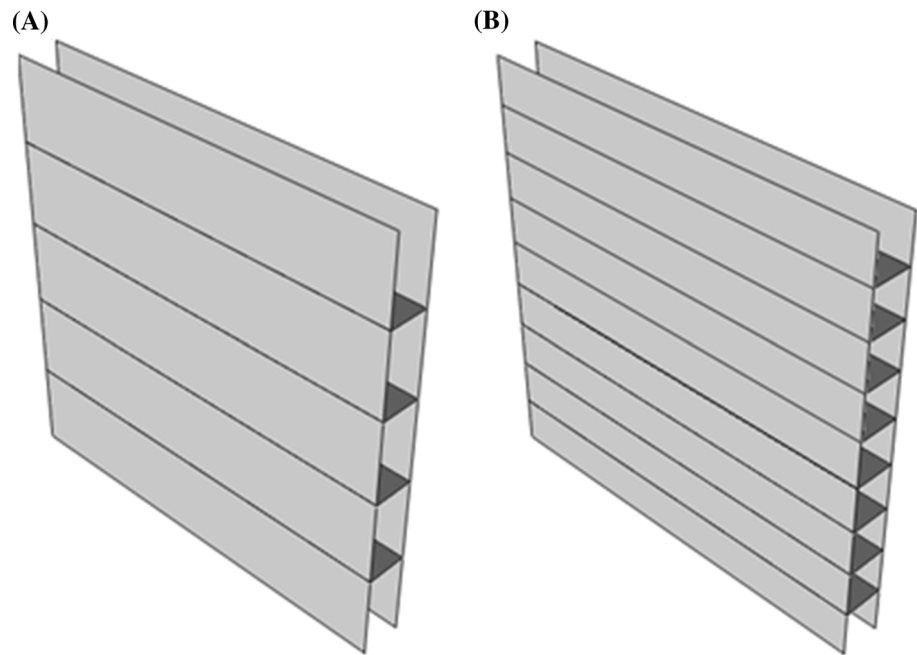


Fig. 2 Plastic property

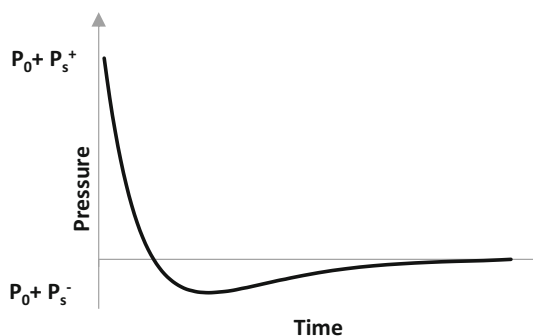


Fig. 3 Blast pressure time-history

in standoff distance. The effect of front cover plate thickness on the midpoint deflection is more important than that of the back plate. Increasing the core thickness and corrugation angle improved the performance of panel with a lower deflection, while increasing the core height led to a

larger localized deflection at the front plate and a lower displacement of back cover plate (Zhang et al. 2015).

In recent years, some researchers have focused on complicated or multihazard scenarios including underwater explosion (Mori et al. 2009), effects of extreme temperatures on blast response of sandwich structures (Tasdemirci et al. 2016; Fahr et al. 2016), combined shock and projectile impact (Ebrahimi et al. 2016), combined blast and fragment loading (Zhang et al. 2017) and multiple intense shocks (Ebrahimi and Vaziri 2013).

The mechanical response and fracture of metallic sandwich panels subjected to multiple impulsive loads were investigated for panels with honeycomb and folded plate core by Ebrahimi and Vaziri (2013). The performance when subjected to multiple blast loads is quantified by the maximum displacement of the cover plates and the core strain. According to results, the panels with a relative core density of 4–5% have minimum cover sheet displacement. Results also show that sandwich panels perform better than solid plates with same weight and material. For panels clamped at their boundary, the failure mechanisms are core failure, face failure and tearing at the boundary (Ebrahimi and Vaziri 2013).

It should be noticed that in different scenarios such as battle, terroristic attacks and even fire conditions in certain infrastructures, the structures are subjected to multiple consecutive blast scenarios, and therefore, the influence of iterative blast loads on the structures and structural response to such scenarios can be very important. Although large numbers of reports on blast-loaded metallic sandwich panels and their dynamic responses can be found in the

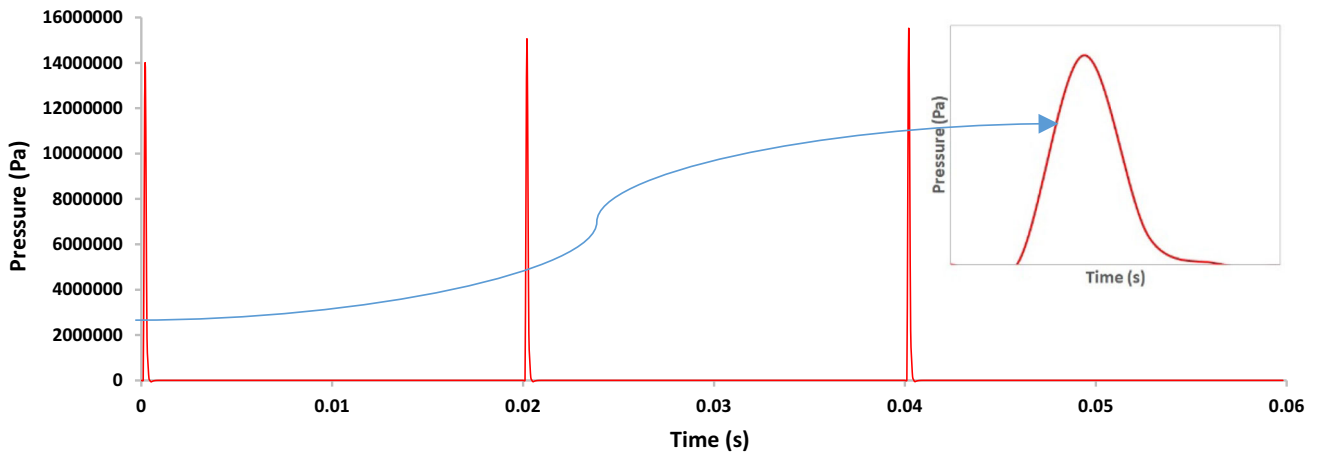


Fig. 4 Time-history of ConWep blast pressure

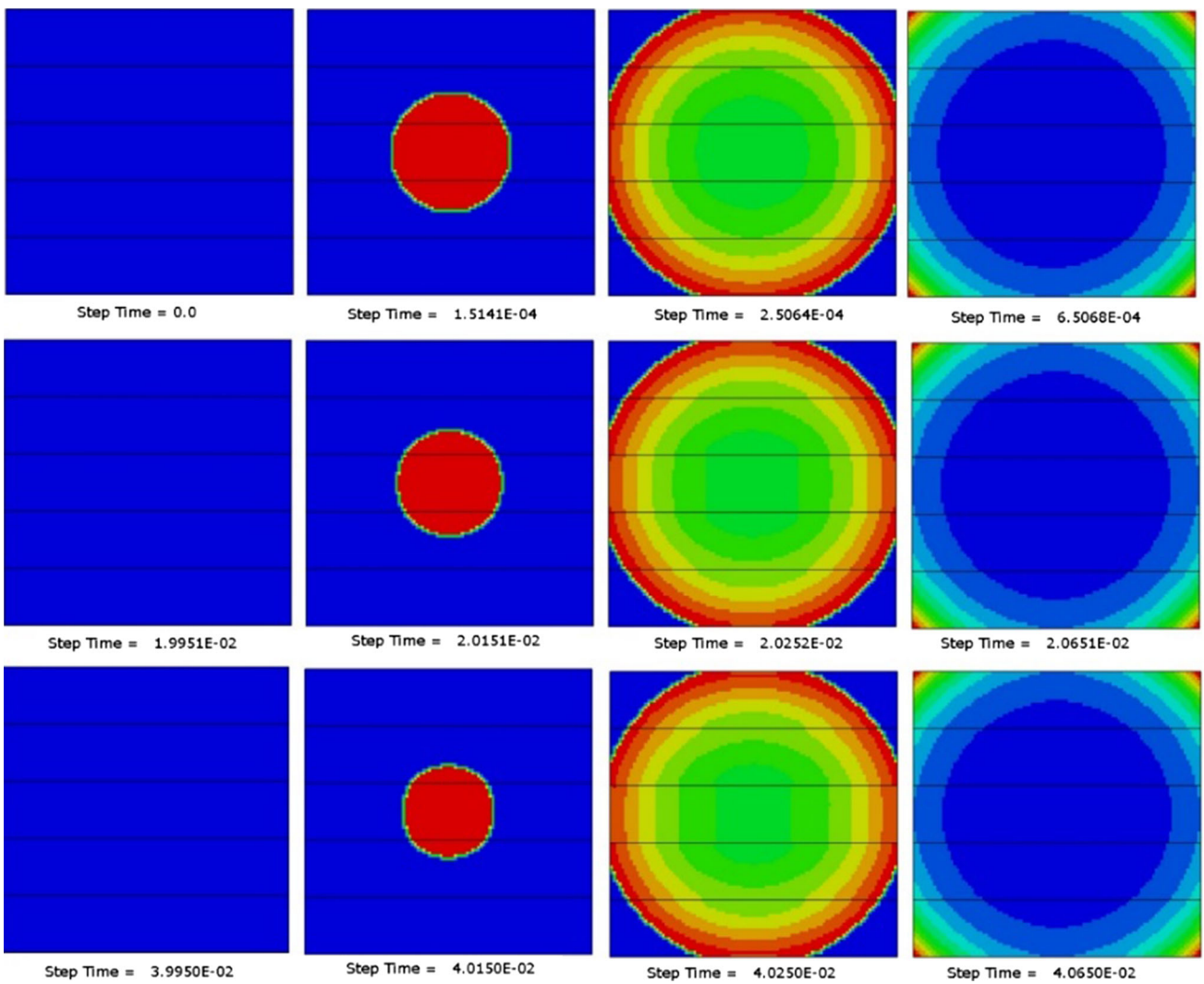


Fig. 5 Time-dependent non-uniform distribution of ConWep blast pressure on the front face of the sandwich panel

literature, the effects of multiple blast loads on dynamic response, deflection and energy dissipation capacity of

I-core sandwich structures are not well understood. In this paper, the nonlinear dynamic response of steel I-core

Table 1 Comparison of experimental and numerical results

<i>S</i>	<i>t</i> (m)	<i>D</i> (m)	<i>W</i> (kg TNT)	<i>R</i> (m)	δ/t (experimental ^a)	δ/t (numerical, LS-DYNA ^a)	δ/t (numerical, Abaqus ^b)
2	0.02	1	3.75	0.2	2.70	2.62	2.50
4	0.01	0.5	0.468	0.1	2.60	2.59	2.46
2	0.02	1	8.75	0.2	5.35	5.24	5.83

^aAs presented by Neuberger et al. (2007)

^bPresent study

sandwich panel under three multiple consecutive blast scenarios using five different explosive charges is numerically investigated. Numerical results are compared with available experimental data to verify the developed FE model. Special emphasis is placed on the evaluation of midpoint displacements of cover plates and energy dissipation of different part of the panels. The results provide useful insight into the dynamic response and energy absorption of steel I-core sandwich panels subjected to multiple consecutive blast scenarios.

2 Finite Element Modeling and Analysis

2.1 Geometry of Panels

The dimensions of numerical models are $1 \times 1 \text{ m}^2$. The overall assembly of model structures is shown in Fig. 1. Thickness of cover plates is 0.008 m. Two arrangements are considered for core elements; while model 1 has 4 core plates, model 2 has 8 core elements. The thickness of core elements for model 1 and model 2 is 0.002 m and 0.001 m, respectively. Therefore, both models have identical weight. The distance between two cover plates is 0.1 m.

2.2 Material Property

Both cover plate and core element are made of steel plates. A multilinear elastic–plastic model with rate-dependent hardening is used for material definition. The model assumes von Mises plasticity with isotropic hardening. The elastic part is defined by Young’s modulus and Poisson’s ratio. The plastic part is defined as the true stress and plastic strain. Abaqus calculates values of yield stress from the current values of plastic strain and approximates the stress–strain behavior of steel with a series of straight lines joining the given points to simulate the material behavior. In this study, multilinear curve is used. The material behaves as a linear elastic up to the yield stress, and after this stage, it goes into the strain hardening stage until reaching the ultimate stress. In this paper, the yield stress of all models is 300 MPa and Young’s modulus is 210 GPa. Poisson’s ratio is 0.3, and the density is 7850 kg/m^3 . The

plastic part is defined using multilinear curve as shown in Fig. 2.

In the case of high-rate loading such as blast and impact, strain-rate dependency is very important; therefore, strain-rate effects are included by adjusting the material dynamic yield stress according to Eq. 1 (Kurtaran et al. 2003).

$$\sigma_y = \sigma_0 \left[1 + \left| \frac{\dot{\epsilon}}{D} \right|^{\frac{1}{n}} \right] \quad (1)$$

where σ_y and σ_0 are dynamic and static yield stresses and $\dot{\epsilon}$ is strain rate. D and n are experimental constants. On the basis of this relation, static and dynamic yield stress ratio depends on deformation speed. In this paper, values for D and n are: $D = 40 \text{ s}^{-1}$ and $n = 5$ (Kurtaran et al. 2003).

2.3 Blast Loading and Boundary Condition

The threat for the conventional bombs is defined by two basic parameters: charge weight and the standoff distance. As shown in Fig. 3, time-history of blast pressure of conventional bombs is divided into a positive phase and a negative phase. In the first phase, maximum overpressure, P_s^+ , is developed suddenly and decays to atmospheric pressure, P_0 , in the time T^+ . For the negative phase, the maximum pressure, P_s^- , has lower amplitude and longer duration (T^-). The pressure time-history in Fig. 3 can be approximated by Eq. 2 (Ngo et al. 2007).

$$P(t) = P_s^+ \left(1 - \frac{t}{T^+} \right) e^{-\frac{bt}{T^+}} \quad (2)$$

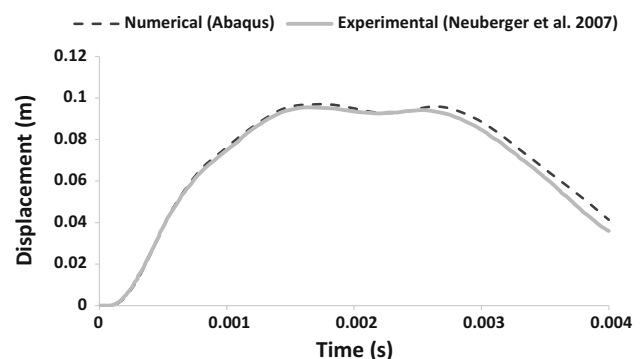
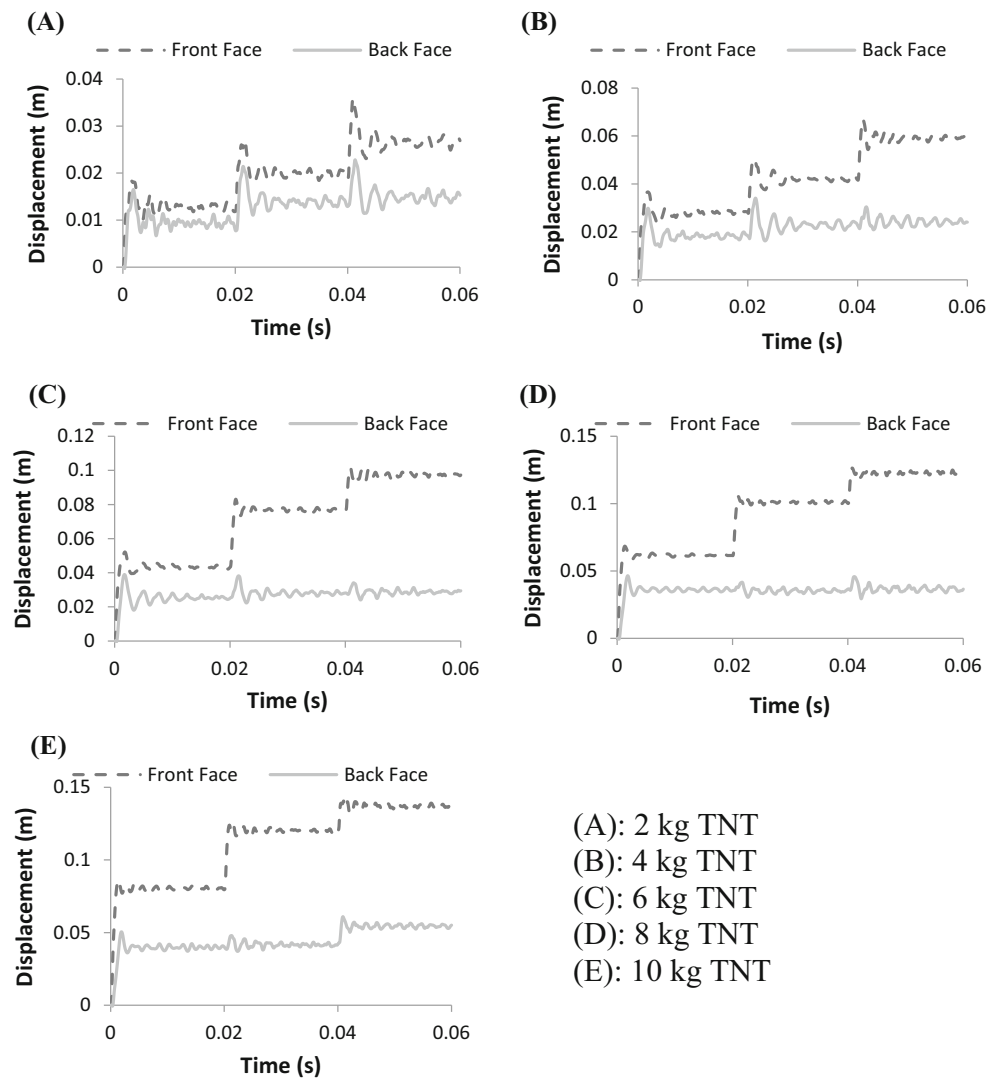


Fig. 6 Comparison of displacement time-history

Fig. 7 Midpoint displacements time-history of model 1 under different blast loads



where $P(t)$ is overpressure at time t , P_s^+ is maximum over pressure, and b is an experimental constant.

In Abaqus/Explicit, the ConWep model can be used for air blast loading on structures. The loading effects due to blast in air can be defined by empirical data provided by the ConWep model in conjunction with the incident wave loading definition. The ConWep model uses a scaled distance based on the distance of the surface from the source of the blast and also the explosive charge weight (Simulia 2010). In ConWep, the total pressure on a surface due to the blast wave is a function of the incident pressure, the reflected pressure and the angle of incidence. The total pressure is defined by Eq. (3) (Simulia 2010).

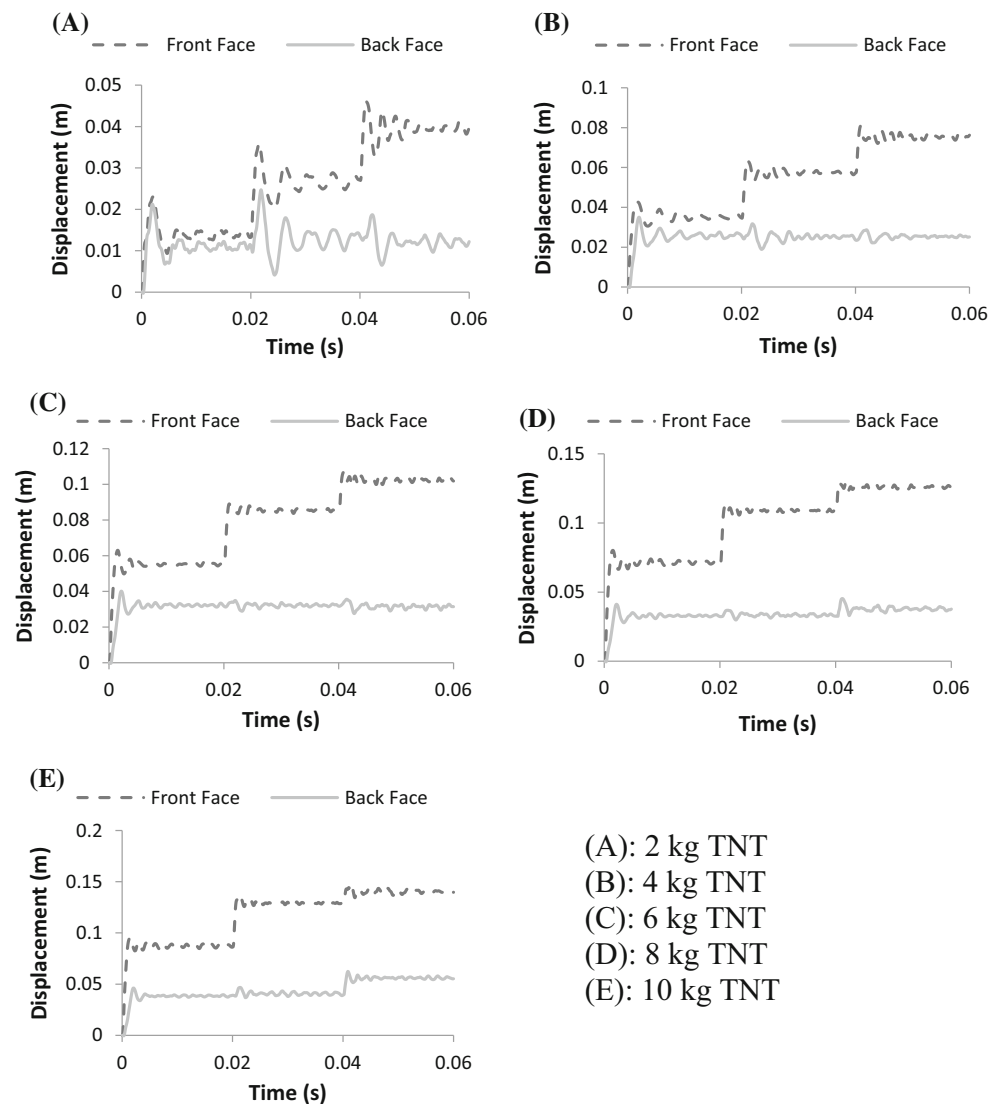
$$P(t) = P_{\text{incident}}(t) [1 + \cos(\theta) - 2 \cos^2(\theta)] + P_{\text{reflect}}(t) \cos^2(\theta) \quad (3)$$

where $P(t)$ is total pressure, $P_{\text{incident}}(t)$ and $P_{\text{reflect}}(t)$ are incident pressure and reflected pressure, respectively, and θ

is angle between the normal of the loading surface and the vector that points from the surface to the explosion source.

In this paper, five different values of explosive charges (2, 4, 6, 8 and 10 kg TNT) are used. The standoff distance is 0.5 m for all models and charges. Loading time-history is considered so that simulate three multiple consecutive blast scenarios. The interval between each consecutive blast is 0.02 s. The explosive charges are selected based on the weight of small terrorist bomb (pipe bomb or briefcase bomb) and/or land mines. Consecutive blast interval is chosen in a way that the vibration of previous blast does not interfere with the response of the structure under next blasts. ConWep model produce time-dependent non-uniform distribution of blast pressure on the target surface. Figure 4 shows blast pressure time-history for model 1 when 2 kg explosive charge is applied. Slight differences between peak overpressures are due to the deformation of front plate under previous blasts. Figure 5 shows time-

Fig. 8 Midpoint displacements time-history of model 2 under different blast loads



dependent distribution of blast pressure on front face of model 1.

Clamped boundary conditions are used for both models in all of the numerical analysis. The boundary conditions are applied to both cover plates.

2.4 Finite Elements and Analysis Approach

Abaqus/Explicit is used for numerical analysis. The fourth noded doubly curved shell element, S4R, is used to model cover plates and core's elements. The S4R is a general-purpose, quadrilateral, stress/displacement shell element with reduced integration, a large-strain and enhanced hourglass control (Simulia 2010). While using reduced integration, S4R is very robust and suitable for a wide range of applications and successfully used in structures under extreme loadings (Imbalzano et al. 2016, 2018). Although there is no evidence that hourglassing is a

considerable problem in the analysis (by comparing artificial strain energy to internal energy), hourglass control is employed in the analysis. The influence of material damping is not considered in this study because damping has little importance in controlling the maximum response of structures subjected to blast loads (Chopra 1995).

3 Finite Element Validation

In order to validate the present numerical model, a circular plate subject to blast loads as described by Neuberger et al. (2007) is considered. The plate has a radius of 1 m and a thickness of 0.05 m. The density of the material is 7850 kg/m^3 , Young's modulus is 210 GPa, and Poisson's ratio is 0.28. The plastic property is modeled with an isotropic hardening bilinear model, with yield stress of 1000 MPa and hardening plastic modulus $E_p = 2 \text{ GPa}$.

Explosive charge is 50 kg TNT and located 0.5 m directly above the center of the plate. The TNT charges were hanged in air using fisherman’s net and were ignited from the center of the charge. The explosive test was performed for two scale factors: $S = 2$ and $S = 4$. An explicit non-linear dynamic analysis is performed for a period of 4 ms. The S4R elements with sufficient fine mesh size are used in finite element modeling. Clamped boundary conditions are applied to the plate. Midpoint displacements are used for comparison and verification.

Table 1 shows a comparison between experimental–numerical results presented by Neuberger et al. and obtained numerical results. In this table, S is scale factor and t , D , W and δ are thickness of plate, diameter of model, weight of explosive charge and maximum midpoint deflection under blast loads, respectively. Numerical models show a good agreement with measured test results for maximum displacement, so the multilinear elastic–plastic model has sufficient accuracy for numerical modeling of blast-loaded structures. Comparison of displacement time-histories of numerical and experimental model is shown in Fig. 6.

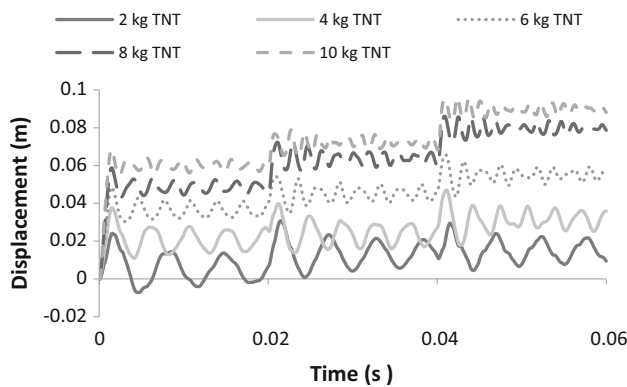


Fig. 9 Midpoint displacements time-history of equivalent solid plate under different explosive charges

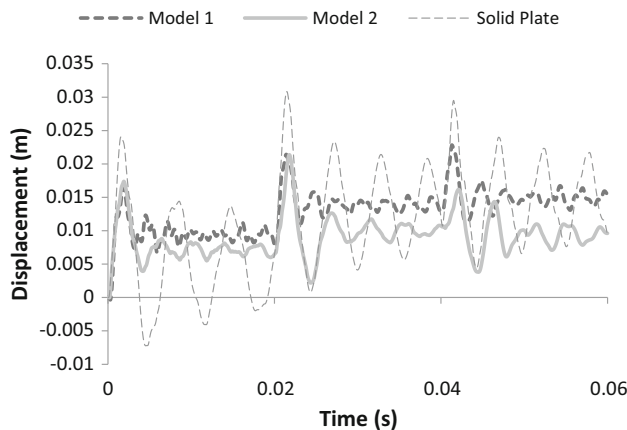


Fig. 10 Displacement time-history under 2 kg TNT

4 Results and Discussion

4.1 Midpoint Displacement

Figure 7 shows midpoint displacements of model 1 under five blast scenarios. As expected, front faces have more deflection than back faces because of energy dissipation in core elements. In general, the differences between displacements of two face plates increase as charge weight increases. When 2 kg TNT is applied, midpoint node vibrated and reached a peak displacement of 35 mm for front face and 22 mm for back face. In this case, the difference between deflections of front face and back face is not considerable in first or second blast, because explosive charge is not enough to use complete plastic dissipation capacity of sandwich structure, but for 6 kg TNT or more, differences between deflection of front face and back face are considerable even at first blast.

Figure 8a–e shows midpoint displacements of model 2 when subjected to mentioned blast loads. In comparison with model 1, model 2 has less midpoint displacement for

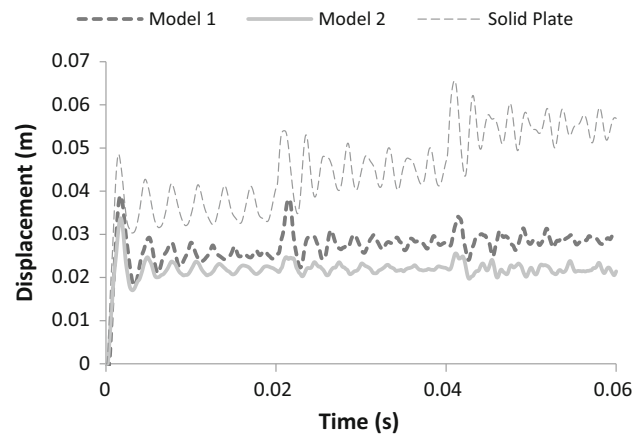


Fig. 11 Displacement time-history under 6 kg TNT

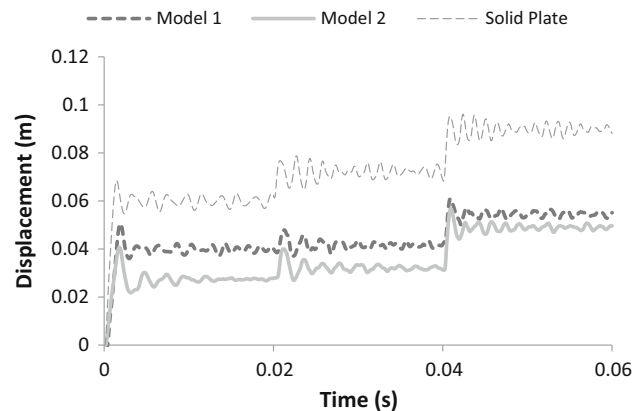


Fig. 12 Displacement time-history under 10 kg TNT

the all blast simulations. This phenomenon is partially because of larger elastic stiffness in I-core due to better distribution of core elements.

Figure 9 shows time-history of midpoint displacement of equivalent solid plate with same material and weight. As illustrated in this figure, sandwich structures have essentially better performance than solid plate. With the increase in blast intensity or number of blasts, this priority is intensified. It should be noticed that in blast-loaded sandwich panels the amplitude of vibration after 0.02 s is negligible, because of high energy dissipation in sandwich structures. In this case, the remained slight oscillation cannot affect the dynamic response after second and third blasts. On the other hand, in blast-loaded plate the vibrations amplitude is not negligible at 0.02 s after each blast and it is necessary to apply second and third blasts at the time before or after 0.02 s to achieve maximum response.

This phenomenon is intentionally neglected in this study, because this change cannot alter the overall response and comparisons remain solid. Figures 10, 11 and 12 summarize displacement time-history of all numerical models under 2, 6 and 10 kg TNT, respectively. Better performance of sandwich structures in comparison with solid plates when subjected to multiple consecutive blasts is visible in these figures. Displacement counters of numerical models under 6 kg TNT are shown in Fig. 13.

Table 2 summarizes maximum deflection under different charges for all numerical models. In this table, superscripts illustrate the occurrence of absolute maximum deflection for each scenario. For all front plates and also for solid plate, the absolute maximum deflection occurs after third blast. (Except for solid plate under 2 kg TNT, the cause has been described.) That means midpoint displacement of front plates increases after each blast. The

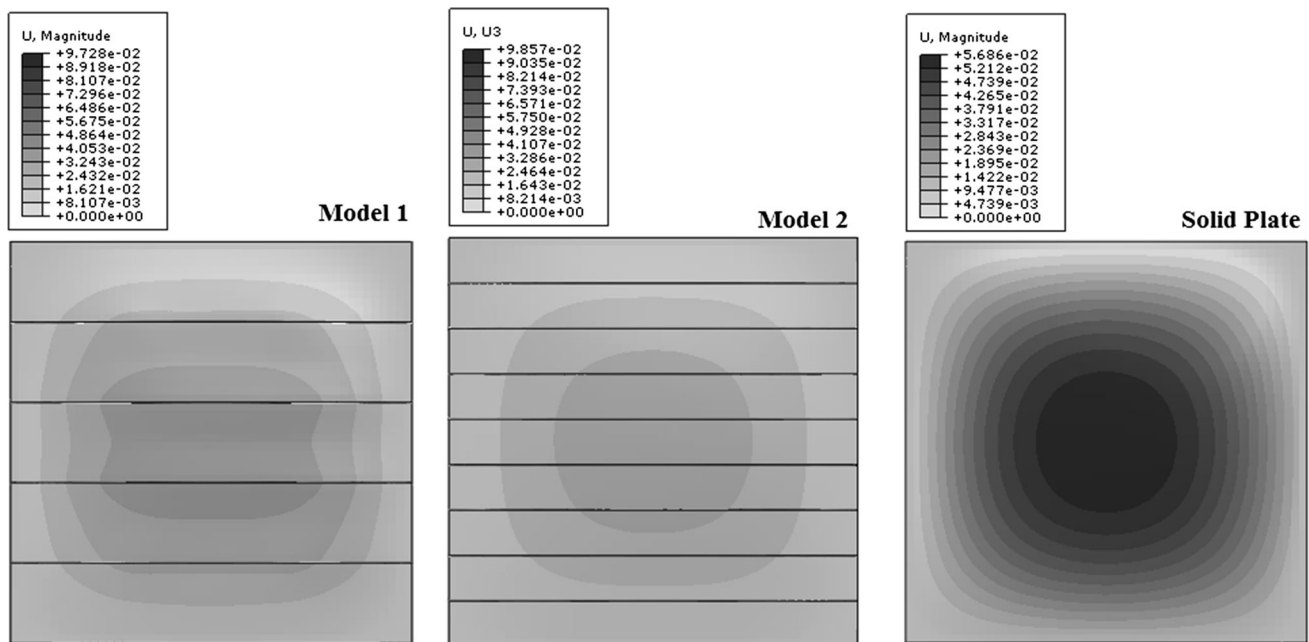


Fig. 13 Displacement counter of model structures under 6 kg TNT at the end of the analysis

Table 2 Maximum deflection under different charge weights

Charge weight	Model 1		Model 2		Solid plate
	Front face	Back face	Front face	Back face	
2 kg TNT	0.035 ^c	0.022 ^c	0.038 ^c	0.021 ^b	0.030 ^b
4 kg TNT	0.066 ^c	0.034 ^b	0.076 ^c	0.027 ^a	0.047 ^c
6 kg TNT	0.101 ^c	0.038 ^a	0.104 ^c	0.033 ^a	0.065 ^c
8 kg TNT	0.126 ^c	0.046 ^a	0.121 ^c	0.044 ^c	0.086 ^c
10 kg TNT	0.0140 ^c	0.060 ^c	0.135 ^c	0.056 ^c	0.096 ^c

^aPeak occurs after first blast
^bPeak occurs after second blast
^cPeak occurs after third blast

rate of increase is mainly dependent on the state of deformation in I-core. On the other hand, for back plate, maximum absolute deflection occurs at second or third blast for lower blast load. With the increase in charge weight, the absolute maximum deflection will occur at first blast (model 1 under 6–8 kg TNT and model 2 under 4–6 kg TNT). Depending on the models configurations, after specific blast load (charge weight), the absolute maximum deflection of back plate occurs again after third blast (e.g., 10 kg TNT for model 1 and 8 kg TNT for model 2). Three different phases in the behavior of sandwich panels under consecutive blast scenarios are observable. In the first phase, deflection of front and back faces is almost

equal, because I-core elements have enough elastic capacity to transfer forces to back face without intense plastic deformations. In the second phase, core's element start to considerable plastic deformation (but not crushing and direct contact between two cover plates) and most of the blast energy dissipated in front face and I-core elements by plastic dissipation, as results deflection of back plate is negligible in comparison with front plate. In the third phase, almost complete crushing of core element especially in the middle of the panel is expected and back plate starts to deform because of direct contact between elements and therefore, the deflections of back cover plates increase. Figure 14 shows these three phases schematically.

Fig. 14 Behavior of sandwich panels under consecutive blast scenarios

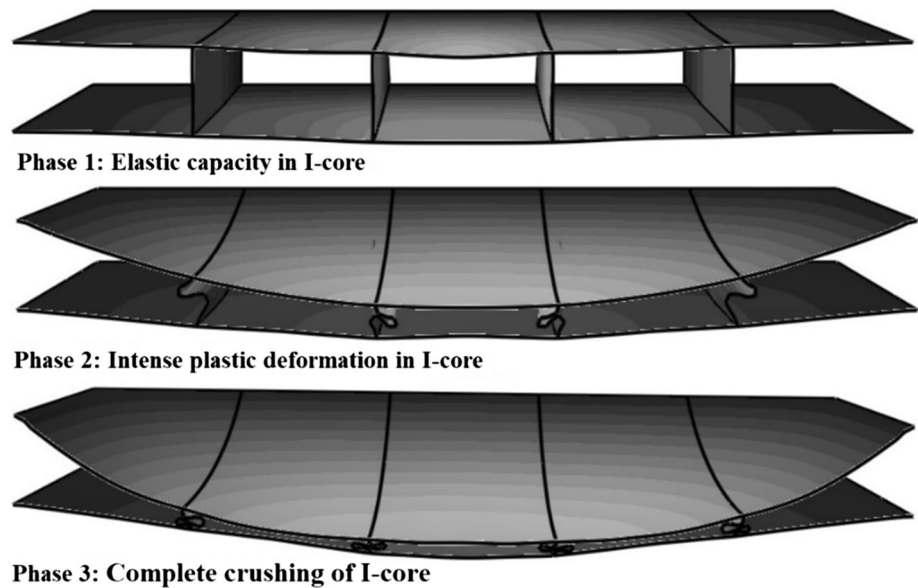
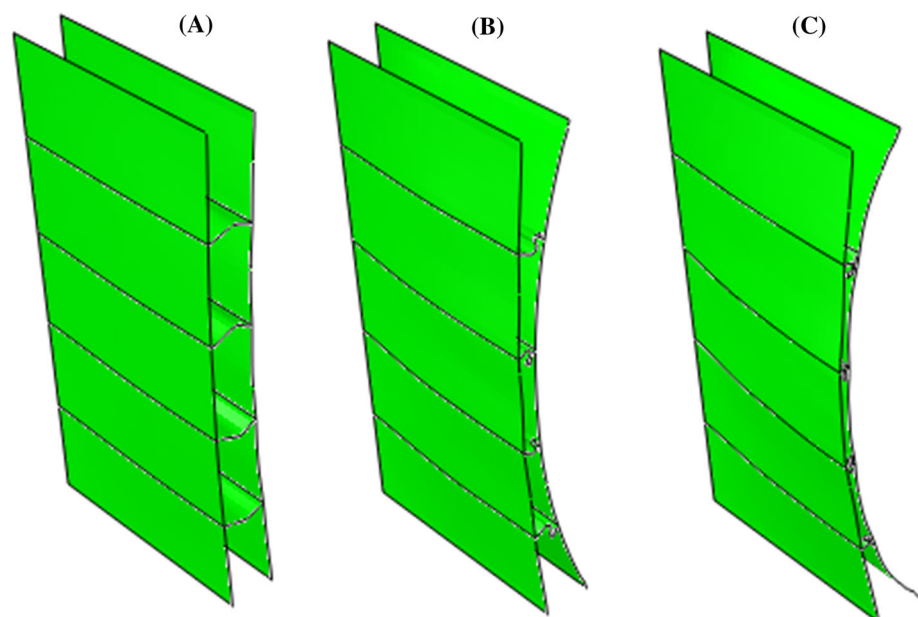


Fig. 15 Cross sections of deformed shapes of model 1 at the end of the analysis **a** under 2 kg TNT, **b** under 6 kg TNT and **c** under 10 kg TNT



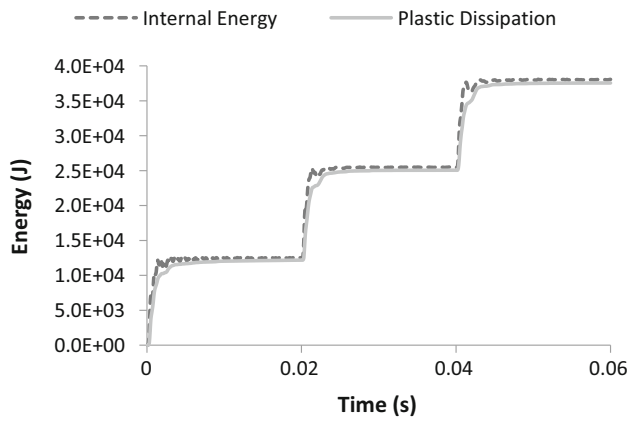


Fig. 16 Comparison of internal energy and plastic dissipation for model 1 under 2 kg TNT

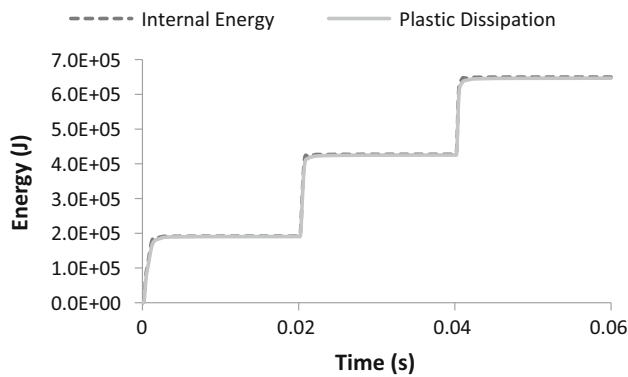


Fig. 17 Comparison of internal energy and plastic dissipation for model 1 under 10 kg TNT

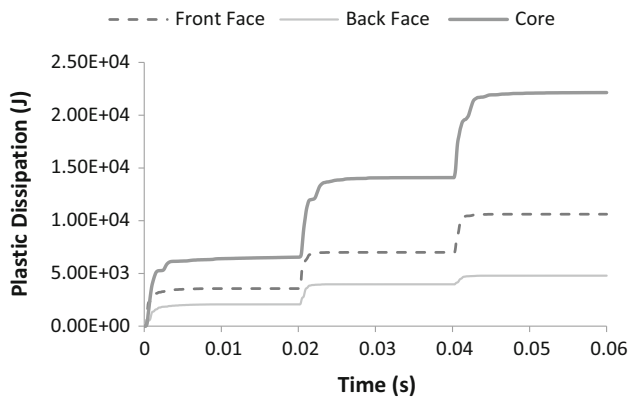


Fig. 18 Plastic dissipation of model 1 under 2 kg TNT

Figure 15 shows deformed cross sections of model 1 under 2, 6 and 10 kg TNT at the end of the analysis.

4.2 Energy Dissipation of the Models

Comparison of the internal energy and the total plastic dissipation shows that most of the energy by the blast loads

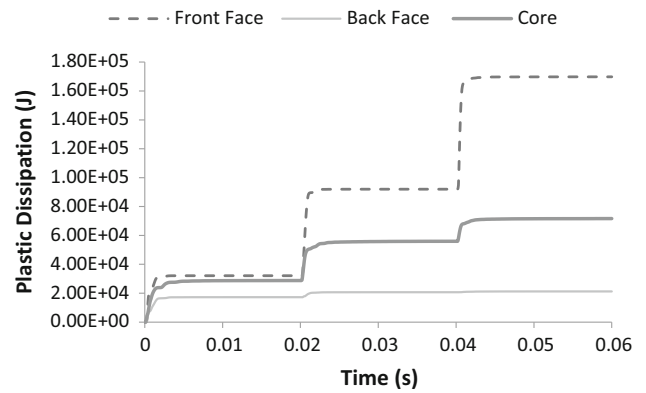


Fig. 19 Plastic dissipation of model 1 under 6 kg TNT

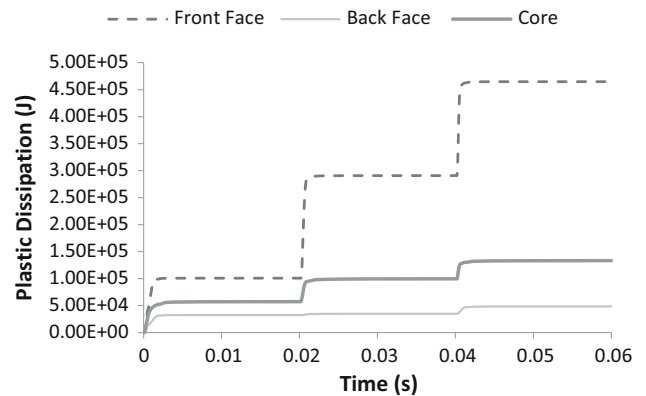


Fig. 20 Plastic dissipation of model 1 under 10 kg TNT

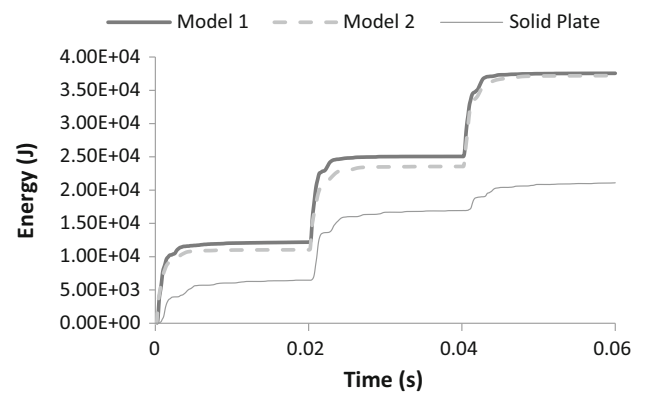


Fig. 21 Total plastic dissipation time-history under 2 kg TNT

is dissipated by plastic deformation even for lower blast loads. With the increase in explosive charge weight, this effect is intensified. Figures 16 and 17 show a comparison of total internal energy and plastic energy time-history for 2 kg and 10 kg explosive charges in model 1. The same results are also observed for model 2.

Figures 18, 19 and 20 compare plastic dissipation in core and face plates for model 1. As shown in these figures, for 2 kg explosive charge, most of the energy dissipation

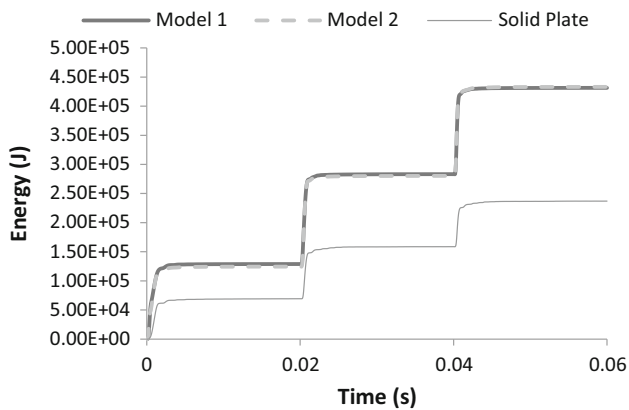


Fig. 22 Total plastic dissipation time-history under 8 kg TNT

occurred in I-core. In this case, back face remains almost elastic. For larger charges, plastic deformation progressively increases in front face that leads to a considerable increase in energy dissipation of front face in comparison with I-core. While plastic deformation is more severe in core elements, the total plastic dissipation is bigger in front face because larger area and more material are in cover plates in comparison with I-core.

Figures 21 and 22 compare total plastic dissipation in numerical models. Energy dissipation in sandwich panels is much larger than solid plate. Dissipation in two sandwich models is almost equal, especially for larger blast loads. It should be noticed that the only difference between two sandwich structures is in their core elements and after the crushing of I-core elements, same plastic dissipation potential is anticipated. With the increase in charge weight and subsequently blast pressure, difference in energy dissipation between plate and sandwich structures is increased.

5 Conclusions

In this paper, the nonlinear dynamic response of steel I-core sandwich panels under three multiple consecutive blast scenarios is investigated using finite element method. Numerical results are compared with available experimental data to verify the developed finite element model, and good agreement is observed. Special emphasis was placed on the evaluation of maximum midpoint deflection of cover plates and energy dissipation of different parts of sandwich panels.

According to results, sandwich panels have essentially better performance than solid plate with the same material and mass when subjected to multiple consecutive blasts. With the increase in blast pressure or number, this priority is increased.

Results also show that midpoint displacement of front plate increased after each blast scenario. On the other hand, for back plate, occurrence of maximum absolute deflections depends on blast pressure and model's configuration. In this regard, three different phases in the behavior of sandwich panel under consecutive blast scenario are observed. In first phase, due to sufficient elastic capacity in core elements, deflection of front and back plates is almost identical. In the second phase, core's element start to considerable plastic deformation and most of the blast energy dissipated in front plate and core element and as results deflection of back plate is negligible. In the third phase, almost complete crushing of core element occurred and back plate starts to deform due to the direct contact between elements. The obtained results provide better insight into the behavior of steel I-core sandwich panel under consecutive blast scenarios.

In this paper, consecutive blast interval is chosen in a way that the vibration of the previous blast does not interfere with the response of the sandwich panels under next blasts. Further study is still required to investigate the effects of interaction between consecutive blasts and its influences on the dynamic response of steel sandwich panels subjected to multiple consecutive blast scenarios.

References

- Andrews EW, Moussa NA (2009) Failure mode maps for composite sandwich panels subjected to air blast loading. *Int J Impact Eng* 36(3):418–425
- Arora H, Del Linz P, Dear JP (2017) Damage and deformation in composite sandwich panels exposed to multiple and single explosive blasts. *Int J Impact Eng* 104:95–106
- Chopra AK (1995) *Dynamics of structures*. Prentice Hall, Englewood Cliffs
- Dharmasena KP, Wadley HN, Xue Z, Hutchinson JW (2008) Mechanical response of metallic honeycomb sandwich panel structures to high-intensity dynamic loading. *Int J Impact Eng* 35(9):1063–1074
- Ebrahimi H, Vaziri A (2013) Metallic sandwich panels subjected to multiple intense shocks. *Int J Solids Struct* 50(7):1164–1176
- Ebrahimi H, Ghosh R, Mahdi E, Nayeb-Hashemi H, Vaziri A (2016) Honeycomb sandwich panels subjected to combined shock and projectile impact. *Int J Impact Eng* 95:1–11
- Fahr P, Yazici M, Shukla A (2016) Shock response of filled corrugated sandwich structures under extreme temperatures. *J Sand Struct Mater*. <https://doi.org/10.1177/1099636216650987>
- Fatt MSH, Palla L (2009) Analytical modeling of composite sandwich panels under blast loads. *J Sandw Struct Mater* 11(4):357–380
- Fleck NA, Deshpande VS (2004) The resistance of clamped sandwich beams to shock loading. *J Appl Mech* 71(3):386–401
- Imbalzano G, Tran P, Ngo TD, Lee PV (2016) A numerical study of auxetic composite panels under blast loadings. *Compos Struct* 135:339–352
- Imbalzano G, Linforth S, Ngo TD, Lee PV, Tran P (2018) Blast resistance of auxetic and honeycomb sandwich panels: comparisons and parametric designs. *Compos Struct* 183:242–261

- Kurtaran H, Buyuk M, Eskandarian A (2003) Ballistic impact simulation of GT model vehicle door using finite element method. *Theor Appl Fract Mech* 40(2):113–121
- Li X, Wang Z, Zhu F, Wu G, Zhao L (2014) Response of aluminium corrugated sandwich panels under air blast loadings: experiment and numerical simulation. *Int J Impact Eng* 65:79–88
- Mori LF, Queheillalt DT, Wadley HNG, Espinosa HD (2009) Deformation and failure modes of I-core sandwich structures subjected to underwater impulsive loads. *Exp Mech* 49(2):257–275
- Neuberger A, Peles S, Rittel D (2007) Scaling the response of circular plates subjected to large and close-range spherical explosions. Part I. Air-blast loading. *Int J Impact Eng* 34(5):859–873
- Ngo T, Mendis P, Gupta A, Ramsay J (2007) Blast loading and blast effects on structures—an overview. *Electron J Struct Eng* 7:76–91
- Nurick GN, Langdon GS, Chi Y, Jacob N (2009) Behaviour of sandwich panels subjected to intense air blast. Part 1. Experiments. *Compos Struct* 91(4):433–441
- Rathbun HJ, Radford DD, Xue Z, He MY, Yang J, Deshpande V, Evans AG (2006) Performance of metallic honeycomb-core sandwich beams under shock loading. *Int J Solids Struct* 43(6):1746–1763
- Remennikov AM, Kong SY (2012) Numerical simulation and validation of impact response of axially-restrained steel–concrete–steel sandwich panels. *Compos Struct* 94(12):3546–3555
- Schiffer A, Tagarielli VL (2014) The one-dimensional response of a water-filled double hull to underwater blast: experiments and simulations. *Int J Impact Eng* 63:177–187
- Shim CS, Yun NR, Shin DH, Yu IH (2013) Design of protective structures with aluminum foam panels. *Int J Steel Struct* 13(1):1–10
- Simulia, Dassault Systèmes (2010) Abaqus 6.10: analysis user's manual. Simulia Corp, Providence
- Tasdemirci A, Kara A, Turan K, Sahin S, Guden M (2016) Effect of heat treatment on the blast loading response of combined geometry shell core sandwich structures. *Thin Walled Struct* 100:180–191
- Vatani Oskouei A, Kiakojouri F (2015) Non-linear dynamic analysis of steel hollow I-core sandwich panel under air blast loading. *Civ Eng Infrastruct J* 48(2):341–362
- Yazici M, Wright J, Bertin D, Shukla A (2014) Experimental and numerical study of foam filled corrugated core steel sandwich structures subjected to blast loading. *Compos Struct* 110:98–109
- Zhang P, Liu J, Cheng Y, Hou H, Wang C, Li Y (2015) Dynamic response of metallic trapezoidal corrugated-core sandwich panels subjected to air blast loading—an experimental study. *Mater Des* 65:221–230
- Zhang C, Cheng Y, Zhang P, Duan X, Liu J, Li Y (2017) Numerical investigation of the response of I-core sandwich panels subjected to combined blast and fragment loading. *Eng Struct* 151:459–471
- Zhu F, Zhao L, Lu G, Wang Z (2008) Deformation and failure of blast-loaded metallic sandwich panels—experimental investigations. *Int J Impact Eng* 35(8):937–951
- Zhu F, Zhao L, Lu G, Gad E (2009) A numerical simulation of the blast impact of square metallic sandwich panels. *Int J Impact Eng* 36(5):687–699